HAL open science

From State Transitions to Sensory Regularity: Structuring Uninterpreted Sensory Signals from Naive Sensorimotor Experiences

Loïc Goasguen, Jean-Merwan Godon, Sylvain Argentieri

To cite this version:

Loïc Goasguen, Jean-Merwan Godon, Sylvain Argentieri. From State Transitions to Sensory Regularity: Structuring Uninterpreted Sensory Signals from Naive Sensorimotor Experiences. 2022. hal-03537409v3

HAL Id: hal-03537409

https://hal.science/hal-03537409v3

Preprint submitted on 28 Sep 2022 (v3), last revised 10 Mar 2023 (v4)

HAL is a multi-disciplinary open access archive for the deposit and dissemination of scientific research documents, whether they are published or not. The documents may come from teaching and research institutions in France or abroad, or from public or private research centers.

L'archive ouverte pluridisciplinaire **HAL**, est destinée au dépôt et à la diffusion de documents scientifiques de niveau recherche, publiés ou non, émanant des établissements d'enseignement et de recherche français ou étrangers, des laboratoires publics ou privés.

From State Transitions to Sensory Regularity: Structuring Uninterpreted Sensory Signals from Naive Sensorimotor Experiences

Loïc Goasguen*, Jean-Merwan Godon* and Sylvain Argentieri

***Abstract*—How could a naive agent build some internal, subjective, notions of continuity in its sensorimotor experiences? This is a key question for all sensorimotor approaches to perception when trying to make them face realistic interactions with an environment, including noise in the perceived sensations, errors in the generation of motor trajectories, or uncertainties in the agent's internal representation of this interaction. This paper proposes a detailed formalization, but also some experimental assessments, of the structure a naive agent can leverage from its own uninterpreted sensorimotor flow to capture a subjective sensory continuity, making it able to discover some notions of closeness or regularities in its experience. The precise role of the agent's actions is also questioned w.r.t. the spatial and temporal dynamics of its exploration of the environment. On this basis, the previous authors' contribution on sensory prediction is extended to successfully handle noisy data in the agent's sensorimotor flow.**

***Index Terms*—Sensorimotor contingencies theory, topological grounding, sensory regularities, uninterpreted sensory signals.**

I. Introduction

It is certainly the case that we deem our sensory experience to be "continuous". Indeed, one crucial property of many psychological perceptual processes is that they generally *seem* continuous [1]; in point of fact, this intuition is strong enough that it is the converse situations where it visibly is not that earn explicit mentions, such as that of Categorical Perception [2], [3]. However, such continuity does not trivially follow from our knowledge of how perceptual processes are materially –e.g. neurally– mediated [4], [5], [6]. In the instance of visual perception, for example, it is known that the eye only acquires very partial snapshots of visual information due to the sparse layout of discrete photoreceptors on its retina as well as the typical trajectories of ocular saccades.

Nevertheless, the continuity of perception subjectively experienced by sensorimotor agents is undeniably useful, allowing for the formulation and exploitation of several powerful ideas. One such idea, for instance, is that of inter and extrapolation. If an agent hopes to infer properties of an unknown situation from a structure it has learned from previous experiences, this agent should have a way to quantify in what way this new experience relates to the data it already knows. One very common way to deal with this is thus to *a priori* assign close properties (e.g. evaluated in terms of distances between sensory signals features, proximity between spatial positions) to experiences that are themselves alike (e.g. by characterizing similar physical properties in the environment, or by rating the system ability to achieve its task): the agent should then have the capabilities to distinguish "similar" things, be it external objects (e.g. a cymbal emitting a sound), sensory attributes (e.g. the intensity, or the tone of the same cymbal), or even sensorimotor capabilities (e.g. the association between theses attributes and the action actually performed by the agent to emit the sound from the cymbal). These capacities may in turn provide grounds for the emergence of its felt continuity of perception: in the end, the agent should then be able to assert that "Red is closer to Pink than it is to Blue, and it is certainly closer to Blue than it is to the sound of a bell" [7]. Such closeness properties are usually leveraged in robotic settings through the well-known mathematical notion of continuity of maps $\mathbb{R}^n \to \mathbb{R}^m$ since the data available to the robotic agent is usually represented numerically. More generally, the modern examination of continuity and related problems is the subject of *topology* [8], a field of mathematics which is precisely devoted to the study of what it means for something to be continuous. This field has indeed proved a powerful tool for bootstrapping [9], or for modeling geometric ideas in several sensorimotor works [10], [11], [12], in particular those that attempt to internally establish properties of external space [13]. Such approaches allow, e.g., motion planning in the internal sensorimotor body representation of an agent through the generation, by interpolation, of continuous motor trajectories [14], or the emergence of a topological representation of the sensor poses from the sensorimotor flow [15]. But importantly, while most of these works are rooted in generic topological intuitions, they all end up exploiting a discrete setup for which most of the topological structures are useless. Indeed, most modern robotic setups rely on discrete time computations for which we can define other tools like distances based on similarities or correlations between elements in the agent's sensorimotor flow. Then, should we want a naive agent to make some kind of judgement about discrete samples by way of its *subjective* sense of continuity, then this sense cannot be entirely grounded in topology; in particular, it cannot be reduced to that of formal continuity. As a consequence, the (almost) only assessments one might provide a naive agent with are entirely categorical: it should then only be able to perform comparisons at a "symbolic" level, denoted by a strict equality operator between e.g. sensory values. While the previous cited contributions certainly prove that these operations allow for the extraction of interesting features or meaningful internal representations from a naive form of sensorimotor flow, they also share limitations related to the absence of the

* Loïc Goasguen and Jean-Merwan Godon have both equally contributed to this paper. All authors are with Sorbonne Université, CNRS, Institut des Systèmes Intelligents et de Robotique, ISIR, F-75005 Paris, France.

aforementioned "closeness" concept: what about their robustness w.r.t. noise, imperfect repetition of motor paths, etc.? The very same limitation is also shared by the previous work by the authors [16]; in this contribution, the interlink between motor actions and sensory prediction is explored, through the demonstration of the existence of a group isomorphism between them. But predicting the sensory outcome of an action is only accessible to the agent by detecting the exact shift of values inside its own sensor array. Endowing the agent with some internal notion of sensory closeness would then make it able to assess its own prediction, and more generally, might allow these sensorimotor approaches to perception –so far mainly restricted to simulated territories– to deal with more realistic conditions.

Importantly, most of the previously cited contributions also claim to deal with uninterpreted sensory signals. But in these works, the form assumed by the signal (and the expected transformations thereof) is usually known and leveraged by the agent; what it ignores instead is *how* these signals relate to the sensorimotor interaction. Then, using a priori distances, metrics, and similarities, maps or representations of the agent's sensorimotor interaction with a generally unknown environment are built [17]. In this paper, however, no "natural" metrics nor algebraic operations on the symbols perceived by the agent are used –in a simular way to [18] where a less formal approach is proposed–, contrary to our understanding of the usual numeric values. This is generally made manifest with the choice to assume that states are coded as numeric values (or tuples thereof), and of special influence with that of whether to use natural (possibly topological, as previously outlined) structures of $\mathbb{R}^N$. Thus, most developments which try to achieve robustness and scalability do so via extrapolation and clustering [12], [14], while [19] goes a bit further by evaluating sensory states similarities by their transition probabilities, but for object identification in a sensorimotor context. Nevertheless, as already argued, most of these techniques require referring to preexisting external metrics, which constitutes assumption about a priori knowledge we would like to avoid.

In this paper, we then propose to examine how some notion of closeness –that we could also relate to some internal notion of *subjective* continuity– in sensorimotor experiences can emerge from uninterpreted sensory information for a naive agent operating in discrete time. To that end, some formal considerations are first introduced in §II. After evaluating a purely topological approach, a metric approach is proposed instead and the probability of transition between sensory symbols is used to define some appropriate notion of sensory distance. On this basis some simple simulations are introduced in Section III to illustrate how an agent could leverage some structure by simply judging if its sensory observations are close or not. This is illustrated for visual perception through the building by a naive agent of the grayscale or some RGB color model. Then, the role of the agent's action in this framework is questioned in §IV. More precisely, the spatial and temporal dynamics of the agent's exploration is shown critical to obtain a meaningful and useful structure of its own sensory symbols. Next, some experiments initially proposed in [16] are reproduced in Section V to illustrate how the proposed framework could allow an agent to actually build some sensory prediction functions even in the presence of sensory noise. Finally, a conclusion ends the paper.

II. Towards a topology of sensory values

This first section aims at defining a topology of sensory values, built on the basis of the agent's sensorimotor experience. After a short subsection devoted to the required definitions and notations, a time variable is added to the formalism in the second subsection, so as to account for the explicit time dependency of the agent's experience, allowing us to introduce a first time-inherited topology. While being possibly sufficient, arguments for the introduction of an explicit metric are then discussed. The third subsection thus proposes the definition of an internal probabilistic metric and highlights the benefits and limits of the proposed approach. Section III then exploits these elements in a simple experimental framework to illustrate these elements and demonstrate their actual exploitation.

A. A short reminder on notations

Let us consider in the following an agent endowed with motor and sensory capabilities. Its internal sensorimotor configuration is classically noted as (**m**,**s**), where $\mathbf{m} \in \mathcal{M}$ (resp. $\mathbf{s} \in \mathcal{S}$) represents the agent's internal motor (resp. sensory) configuration as an element of its corresponding motor $\mathcal{M}$ (resp. sensory $\mathcal{S}$) set. As shown in [16], the agent's motor description can be enriched from $\mathbf{m} \in \mathcal{M}$ to $\mathbf{b} \in \mathscr{B}$, where $\mathbf{b} = (\mathbf{m}, \boldsymbol{\tau})$ depicts the absolute agent's motor configuration. $\mathbf{b}$ is made of the agent's internal (and thus known to it) motor configuration $\mathbf{m}$ and of its absolute external (and thus unknown to it) pose $\boldsymbol{\tau}$ in its ambient space. Importantly, as discussed in [16], switching the motor description from $\mathbf{m}$ to $\mathbf{b}$ allows us to keep a functional relationship between motor and sensory data, even in the case where the agent can freely move in its environment. But while the agent has no direct access to $\mathbf{b}$, it can apply some *motor actions* a on $\mathbf{b} = (\mathbf{m}, \boldsymbol{\tau})$ to go to configurations $\mathbf{b}' = (\mathbf{m}', \boldsymbol{\tau}') = a\mathbf{b}$: the agent knowns instead how to *move* in $\mathscr{B}$. This capability will be exploited later to apply the following developments to get an internal assessment of sensory regularity, see §V. Next, the environment state is characterized as a function $\epsilon : \mathcal{X} \to \mathcal{P}$, i.e. as a state $\epsilon \in \mathscr{E}$ linking the ambient geometrical space $\mathcal{X}$ in which sensorimotor experiences occur (classically endowed with some rigid transformations group $\mathcal{G}(\mathcal{X})$) to the set of the physical properties $\mathcal{P}$ observable by the agent, where $\mathscr{E}$ denotes the set of environmental states. Then, $\epsilon(\mathbf{x})$ represents the observable physical properties at point $\mathbf{x} \in \mathcal{X}$. On the basis of the previous definitions, we can now define the sensorimotor map ψ as the function $\psi : \mathscr{B} \times \mathscr{E} \to \mathcal{S}$, such that $\mathbf{s} = \psi(\mathbf{b}, \epsilon)$. We can notice here that the sensorimotor law does not explicitly depend on time, as is the case of most other contributions in the fields [10], [20], [14]. We will now enrich this formalization with an explicit time dependency. It will then constitute our gateway towards continuity in the sensory experience of the agent. Much like in J. Elman's famous 1990 paper [21] where words are not considered as preexisting categories but more as emergent features in the latent structure of sentences along time [22]. Similarly, the topology of sensory symbols can be considered as the latent structure between them through the sensorimotor experience along time.

B. All is well in continuous land

1) Introducing time in the sensorimotor experience: The definitions we recalled in the previous subsection actually described *snapshots* of the agent's sensorimotor interaction. Nevertheless, these can be easily enriched with an explicit dependency of the various states with a time variable $t \in \mathscr{T}$. Thus, the environmental state $\epsilon \in \mathscr{E}$ can now be written

$$\begin{aligned} \epsilon \colon \mathscr{T} \times \mathcal{X} &\to \mathcal{P} \\ (t, \mathbf{x}) &\mapsto \epsilon(t, \mathbf{x}). \end{aligned} \tag{1}$$

With this notation, we can express an instantaneous snapshot of the environmental state as the partial function

$$\epsilon_t : \mathbf{x} \in \mathcal{X} \mapsto \epsilon_t(\mathbf{x}) = \epsilon(t, \mathbf{x}) \in \mathcal{P}. \tag{2}$$

Therefore, any temporal succession of environment states can be described as a trajectory

$$\gamma_\epsilon : t \in \mathscr{T} \mapsto \epsilon_t \in \mathscr{E}. \tag{3}$$

Correspondingly, the agent's *absolute* configuration trajectories and sensory ones are respectively denoted by

$$\gamma_{\mathbf{b}} : t \in \mathscr{T} \mapsto \mathbf{b}_t \in \mathscr{B}, \tag{4}$$

and

$$\gamma_{\mathbf{s}} = \gamma_{\mathbf{b},\epsilon} : t \in \mathscr{T} \mapsto \mathbf{s}_t = \psi(\gamma_{\mathbf{b}}(t), \gamma_\epsilon(t)) \in \mathcal{S}. \tag{5}$$

In the following, we will consider a particular subset of such temporal environmental, motor, and sensory trajectories representing the set of *effectively valid* trajectories. We thus instead restrict $\epsilon_t \in \mathscr{E}_{\mathscr{T}} \subset \mathscr{F}(\mathscr{T}, \mathscr{E})$ so as to include possible external constraints on the succession in time of physical properties in the agent's environment. In the same vein, one defines $\gamma_{\mathbf{b}} \in \mathscr{B}_{\mathscr{T}}$, where $\mathscr{B}_{\mathscr{T}}$ is the set of all effectively performable motor configurations, possibly allowing to capture e.g. limitations on velocity and their smoothness as actuated by the agent. Consequently, the effectively valid sensory trajectories $\gamma_{\mathbf{s}}$ lie in $\mathcal{S}_{\mathscr{T}}$, with a natural mapping $\mathcal{S}_{\mathscr{T}} \hookrightarrow \mathscr{B}_{\mathscr{T}} \times \mathscr{E}_{\mathscr{T}}$.

2) Towards a sensory topology: Let us now get back to the intuition of the sensory experience being continuous, as discussed in the introduction of this paper. More precisely, this continuity is that of the agent's sensory experience unfolding with the time $\mathscr{T}$ during which it occurs. In (purely) topological settings, an argument examined e.g. in [23] shows that searching for (*formal*) continuity of the $\gamma_{\mathbf{s}}$ sensory experiences is entirely dual to searching for topological constraints on the sensory values $\mathbf{s} \in \mathcal{S}$. These two viewpoints intersect at the *final topology* of the γ_s [8], a topology on $\mathcal{S}$ which precisely encodes which structural constraints on the $\mathbf{s}$ sensory values is needed to make (all) the $\gamma_{\mathbf{s}}$ experiences continuous. While this final topology seems to solve –at least from a purely topological point of view– the initial problem, we have to keep in mind that most robotic setups rely on discrete time computations. The resulting final topology thus makes $\mathcal{S}$ discrete. Intuitively, this occurs because if the agent only experiences jumps in times such that no instant follows continuously from the previous one, then it does not need to introduce new continuities in its sensations to make their succession continuous. So how can we solve this issue? In the following subsection, we propose to switch to metric geometry, which, although less general, might be better suited.

C. Introduction of a statistical sensory metric

Introducing corresponding metric considerations, however, raises new issues: given an abstract sequence of points in a (metrized) point cloud, how can we determine whether it represents a regular/continuous trajectory? For example, how can we decide that a jump in values across a distance of e.g. 5 units corresponds to a *regular* transition, or instead represents a break in continuity? Without *a priori* assumptions about the expected reasonable dynamics of the experience, it seems these numbers are entirely arbitrary, and related to some *external* knowledge that we want the agent to do without. Instead, we propose to define a statistical sensory metric, for which the agent ought to set to zero any distance between sensory values that *immediately* (and not *continuously*) follow one another. Thus, the temporal length between successive sensory samples is now central to how the agent perceives them. Consequently, we should first assume that the agent is able to compute distances (or durations) between two timesteps in $\mathscr{T}$. On this basis, we will assume in all the following that the laws of the sensorimotor experiences the agent can observe are *time homogeneous*. This hypothesis then indicates that no statistical measurement the agent can empirically obtain from its sensorimotor experience may depend on the absolute value of the timestep indexing its interaction. In particular, it should be a natural consequence of the particular choice of timestep being an entirely external convention, implementing a sort of independence of choice of reference.

Let us now define the likelihood $P_{\mathbf{s}'|\mathbf{s}}$ over all experiences that the sensory value $\mathbf{s}'$ immediately follows $\mathbf{s}$ in the sensorimotor flow of the agent along

$$P_{\mathbf{s}'|\mathbf{s}} = \mathbb{P}(\gamma_{\mathbf{s}}(t+1) = \mathbf{s}' \mid \gamma_{\mathbf{s}}(t) = \mathbf{s}). \tag{6}$$

Importantly, from the previous time homogeneity assumption, $P_{\mathbf{s}'|\mathbf{s}}$ does not depend on the current time t it is computed. From there and following the intuition that "closeness" of sensory values $\mathbf{s}$ and $\mathbf{s}'$ should increase whenever the probability of the transition $\mathbf{s} \to \mathbf{s}'$ does, we propose to define a simple metric prototype via

$$\delta_f(\mathbf{s}, \mathbf{s}') = f(P_{\mathbf{s}'|\mathbf{s}}) \quad \forall \mathbf{s}, \mathbf{s}' \in \mathcal{S}, \tag{7}$$

where f should verify the two conditions:

1) $f : [0;1] \to \mathbb{R}_+$: f only needs to map probabilities in $[0;1]$ to nonnegative values, i.e. dissimilarity values;
2) f is non-increasing: probable transitions (i.e. $P_{\mathbf{s}'|\mathbf{s}}$ close to 1) should result in low dissimilarities.

These conditions do not make δ_f a metric since it only verifies the non-negativity property. We therefore extend it via minimal path considerations, i.e., by defining a distance d_f. Let $\mathcal{R}^{\mathbf{s},\mathbf{s}'}$ be the set of all paths from $\mathbf{s}$ to $\mathbf{s}'$, with

$$\langle \mathbf{s} = \mathbf{s}^{(0)}, \mathbf{s}^{(1)}, \ldots, \mathbf{s}^{(k-1)}, \mathbf{s}^{(k)} = \mathbf{s}' \rangle \in \mathcal{R}^{\mathbf{s},\mathbf{s}'}. \tag{8}$$

We can then define d_f along

$$\mathrm{d}_f(\mathbf{s}, \mathbf{s}') = \inf \mathcal{R}^{\mathbf{s},\mathbf{s}'}. \tag{9}$$

This in turn enforces the properties of *triangular inequality* and *reflexivity*. In the case where $\mathcal{S}$ is finite, this reduces to the familiar computational form of finding minimal paths on a finite graph with nonnegative weights (corresponding

to the $\delta_f(\mathbf{s},\mathbf{s}')$ edge from $\mathbf{s}$ to $\mathbf{s}'$). It should also be noted that this does *not* guarantee *symmetry* at its core because $P_{\mathbf{s}'|\mathbf{s}}$ may differ from $P_{\mathbf{s}|\mathbf{s}'}$. Then the δ_f weights naturally define a *directed* graph (*digraph*), which does not impair the search for minimal paths but does however, lead to a non-symmetric d_f function. While there exist several ways to obtain a closely related undirected graph from any given digraph, we hypothesize instead that symmetry should occur as a contingency of the sensorimotor exploration in most real world examples. Therefore, we do not enforce such corrections for now and will instead assess this hypothesis in the resulting graph.

III. Building the sensory topology from statistics

The previous section was devoted to the mathematical roots of the approach. We will now illustrate how these points can be exploited inside a simple experimental framework which could allow a naive agent to leverage a structure on its sensory signals from its own observations. To begin with, a detailed description of the simulation setup is proposed. On this basis, two main experiments are conducted: the first one deals with the construction of a probabilistic sensory metric and the corresponding low-embedding representation for a grayscale camera sensor; the second one extends the reasoning to a more complex representation when using RGB image sensors.

A. Experimental setup and sensory distance estimation

1) Experimental setup: In all the following, we consider an agent endowed with a camera sensor observing a 3D scene. Since we are for now dealing with sensory values and their transitions only, the visual perception is basically simulated by playing a video file $\mathbf{v}[n]$ of size $W \times H$, where n represents the video frame number. This is a (temporary) very restrictive setup, which will be enriched later when discussing the influence of the movement of the agent (see §IV). Also, the experience occurs in discrete time, for which each timestep verifies $t = t_n = nT_s$ with T_s the sampling period. In practice, we have $\mathbf{v}[n] = (v_{ij}[n])_{i,j}$, with $i \in [0; W-1]$, $j \in [0; H-1]$, and where $v_{ij}[n]$ depicts the pixel value of the video at frame n, row i and column j. Each pixel $v_{ij} = (R_{ij}, G_{ij}, B_{ij})$ is represented as a traditional color tuple $\in [\![0; 255]\!]^3$. The agent's sensory state $\mathbf{s}[n]$ is then simulated by applying some instantaneous function $g : [\![0; 255]\!]^3 \to \mathcal{S}$ to the video, i.e.

$$\mathbf{s}[n] = (s_{ij}[n])_{i,j}, \text{ such that } s_{ij}[n] = g(v_{ij}[n]), \tag{10}$$

where $s_{ij}[n]$ represents the (i,j) sensel value at time n, row i and column j of the agent's camera sensor. Introducing $g(.)$ in (10) allows to explain formally how a physical state of the environment (which can be envisaged here as the pixel values of the video) is turned into the internal sensory state of the agent. But one has to keep in mind that the agent does not know the relation (10), it does not even have any knowledge about the meaning of these numerical values: they are only *uninterpreted symbols* to it, with no a priori structure, order, nor any way to actually *compare* them. In addition, the set $\mathcal{S}$ may well be isomorphic to the set of actual pixel values, but there may also have a lower number S of symbols than pixel values, resulting in a compressed representation. Without loss of generality, $\mathcal{S}$ will then be defined as the finite set of positive integers $\{0, \dots, \mathsf{S}-1\}$ with $\mathsf{S} = \mathrm{Card}(\mathcal{S})$, where each sensory symbol $\mathbf{s}_k \in \mathcal{S}$ can equally be written directly as the integer k, and we will adopt a traditional $s_{ij} \in [\![0; \mathsf{S}-1]\!]$ coding convention for the numerical values of each (i,j) sensel, with $\mathsf{S} = 256$ for traditional camera sensors. As outlined in §II-C, it is then proposed to look at the relationship between those S uninterpreted (numerical) symbols through the statistics of their transitions. Let us now detail how these transitions are actually captured.

2) Description of the experiment: In all the following, we will assume that all $W \times H$ agent's sensels contribute equally to the building of the same representation, i.e., all sensels share the same excitation function linking the environment state to the agent's sensations as written in Equation (10). Then, we define a $\mathsf{S}\times\mathsf{S}$ matrix $M = (m_{kl})_{k,l}$ counting all the transitions of sensel values along observations, with

$$m_{kl}[n+1] = m_{kl}[n] + \sum_{i,j} \zeta_{kl}(i,j)[n], \tag{11}$$

with $(i,j) \in [\![1; W \times H]\!]^2$, $m_{kl}[0] = 0$, and k, l both represent two symbols in $\mathcal{S}$ (that is, sensor output values $\mathbf{s}_k$ and $\mathbf{s}_l \in \mathcal{S}$). $\zeta_{kl}(i,j)[n]$ aims to capture the existence of a change of value of the (i,j) sensel from value k at time n to value l at time $n+1$, i.e.

$$\zeta_{kl}(i,j)[n] = \begin{cases} 1 & \text{iff } s_{ij}[n] = k \text{ and } s_{ij}[n+1] = l, \\ 0 & \text{otherwise.} \end{cases} \tag{12}$$

From (11), we can then compute the probability of transition of sensels values gathered in a $\mathsf{S}\times\mathsf{S}$ matrix $P = (p_{kl})_{k,l}$ with

$$p_{kl}[n] = \frac{m_{kl}[n]}{\sum_{q=0}^{S-1} m_{kq}[n]} \tag{13}$$

the probability at time n for any sensel to see its value changing from symbol k to l. Obviously, $p_{kl}[n]$ is expected to converge towards $P_{\mathbf{s}_l|\mathbf{s}_k}$ as time n tends to infinity. Then, once the estimation of the matrix P has converged after a fixed number frames N, it is turned into a $\mathsf{S} \times \mathsf{S}$ metric prototype matrix $\Delta = (\delta_{kl})_{k,l}$ according to Eq. (7) where $f = -\log$[1] is selected, with

$$\delta_{kl} = -\log(p_{kl}[N]). \tag{14}$$

Again, any function verifying the two conditions in §II-C could have been selected. Then, Dijkstra's algorithm [24] is applied to the Δ matrix along Eq. (9) to produce the $\mathsf{S} \times \mathsf{S}$ distance matrix $D = (\mathrm{d}_{kl})_{k,l}$, providing the agent with the result metric d we set out to discover

$$\mathrm{d}_f(\mathbf{s},\mathbf{s}') = \mathrm{d}_{-\log}(\mathbf{s}_k, \mathbf{s}_l) = \mathrm{d}_{kl}, \tag{15}$$

which is finally visualized in 2D or 3D through a multi-dimensional scaling projection method (MDS [25], [26], [27] or ISOMAP [28]).

B. Results for a grayscale perception

The $W \times H = 856 \times 480$ video used to conduct the experiments comes from a slightly stabilized camera filming

[1] If a probability of transition is equal to 0, the corresponding distance is set to `NaN` by convention.

an evening walk in Midtown New York City in the rain[2]. It consists of a natural city scene filmed in real time from a first-person point of view. A grayscale (cropped) preview of the video is shown in Figure 1a. It is clear that this environment exhibits some nice local temporal and spatial continuity properties: the values of each pixel change smoothly in time, while local pixel values are highly correlated. While these are some nice properties to illustrate the building of the sensory topology from statistics, the importance and formalization of these hypotheses w.r.t. the agent's movement capabilities is discussed in §IV.

To begin with, we will consider a function g, mapping the (R_{ij}, G_{ij}, B_{ij}) color coding of the video pixels v_{ij} to the sensel values $s_{ij} \in [\![0; 255]\!]$ of the agent, such that

$$s_{ij} = g(v_{ij}) = h(\texttt{round}(\texttt{mean}(R_{ij}, G_{ij}, B_{ij}))), \qquad (16)$$

where h is a function that can be tuned to artificially modify the agent's perception. Note that g acts here like an excitation function, and is thus supposed to be identical for all sensels. Two cases for h are discussed in the following: either $h() = \mathrm{id}()$ in §III-B1, corresponding to the case where the agent's grayscale perception exactly matches the grayscale version of the video, or $h() = \mathrm{sawtooth}()$ for which the perception is altered on purpose to exhibit the folding of the agent's internal representation between black and white pixel values in the video, as detailed in §III-B2.

1) First case: $h()$ is the identity function:

a) Estimation of the probability of transition between symbols: Since $h() = \mathrm{id}()$ in Eq. (16), the agent's sensory values are made of $\mathsf{S} = 256$ uninterpreted symbols, whose values along frames can be used to compute their probability of transition along Equation (13). The resulting $\mathsf{S} \times \mathsf{S}$ matrix P is shown in Figure 1b and 1e after $n = 5$ and $n = 10^4$ successive sensory transitions respectively. Note that the S symbols are ordered in the figure according to their numerical values: this is something the agent cannot actually do for now, but this ordering has no effect on the reasoning and helps in understanding the process. From Figures 1b and 1e, we can see that the most probable transitions are all placed along the diagonal of the matrix P, meaning that the most probable sensory output at the next time step is the very same symbol, even at the very beginning of the experiment with $n = 5$. Further, the *a priori* ordering of symbols allows to observe that the diagonal is thick and fades away as the symbols values are distant: this clearly indicates that the most probable transitions are the ones to symbols that have *close colors, from an external point of view* (again, the a priori ordering is unknown to the agent). Conversely, the least probable transitions are the ones to *distant* symbols. Those results are in accordance with the intuition that close time intervals lead to close sensory outputs, and that some regularity of the sensory experience has been captured. Note that since the probability estimation is evaluated on occurrences, the case where no transitions at all between two symbols are observed leads to a probability of 0 (represented in white in Figure 1b); this appears at the beginning of the experiment only (see Figure 1e for $n = 10^4$) and mainly concerns *distant* symbols with a very low transition probability, i.e., in the two corners of Figure 1b.

[2]https://youtu.be/eZe4Q_58UTU by courtesy of Nomadic Ambience.

b) Computation of the distance matrix: On the basis of the previous probability of transitions between symbols, we can compute the metric prototype in the form of the $\mathsf{S} \times \mathsf{S}$ matrix Δ whose elements are given by Eq. (14). Then, Dijkstra's algorithm [24] is performed on Δ to obtain the $\mathsf{S} \times \mathsf{S}$ distance matrix D. The resulting matrix D is represented in Figure 1c and 1f for $n = 5$ and $n = 10^4$ respectively. Obviously, one should note that when direct transitions between symbols are missing in P (and thus in Δ) as shown in Figure 1b, Dijkstra's algorithm will nonetheless generally find an alternate path towards those symbols by finding adequate successive transitions; consequently the D matrix is expected to be fully defined (i.e. with all coefficients finite) as long as the agent has experienced enough sensory symbols transitions. This is exactly what is shown in Figure 1c, where the corresponding distance matrix D shows distances between all sensory symbols, while transitions between some of them have not been directly observed yet. We can also see from both Figures 1c and 1f that previous low transition probabilities are now associated with high distances (and vice versa). In addition, we recognize the same diagonal pattern, which now corresponds to low distances. We can also see that D is *almost* symmetric, except in the corners, where lie most of the high distances, corresponding to the least probable transitions of sensory symbols. This is not an encoded property of the agent's experience but instead seems to appear as a contingency of the sensorimotor exploration, as outlined in §II-C. Finally, a qualitative comparison between the two D matrices obtained at the beginning (Figure 1c) and at the end (Figure 1f) of the experiment shows that the very same structures (symmetry, diagonal pattern) are captured very quickly. This is certainly thanks to the identical contribution of all pixels to the building of the same statistic, as one time step actually captures $W \times H \approx 4.10^5$ sensory transitions.

c) Visualization of the representation: Finally, we can qualitatively assess the shape of the captured sensory symbols topology by projecting the resulting distance matrix D into a space of lower dimension. The 2D visualization of the matrix D through a MultiDimensional Scaling (MDS) projection is represented in Figures 1d and 1g. Note that such a method requires the input matrix to be symmetric; hopefully, we qualitatively showed it was almost the case so that MDS can be actually applied on the symmetrized matrix $1/2 \times (D + D^T)$. In both Figures 1d and 1g, each circle represents a single symbol where the inner color corresponds to the color perceived from an external point of view (color that also matches the classical gray-level scale in this case, since $f = \mathrm{id}()$). We can see from this representation that the obtained manifold is almost one-dimensional and captures the classical gray scale from white to black in a continuous manner, even at the very beginning of the experiment. This can be evaluated by looking for the 2 nearest neighbors of each symbol in the internal metric (i.e. with the neighbors computed on D and not on the representation); these neighbors are then linked together in the projection by a line drawn in the figure. Browsing the manifold by following these lines allows to go from white (coded as the number 255) to black (coded as a 0) almost without any discontinuity in the symbol order at the end of the experiment. Interestingly, we can see that the projection obtained at the early stage of

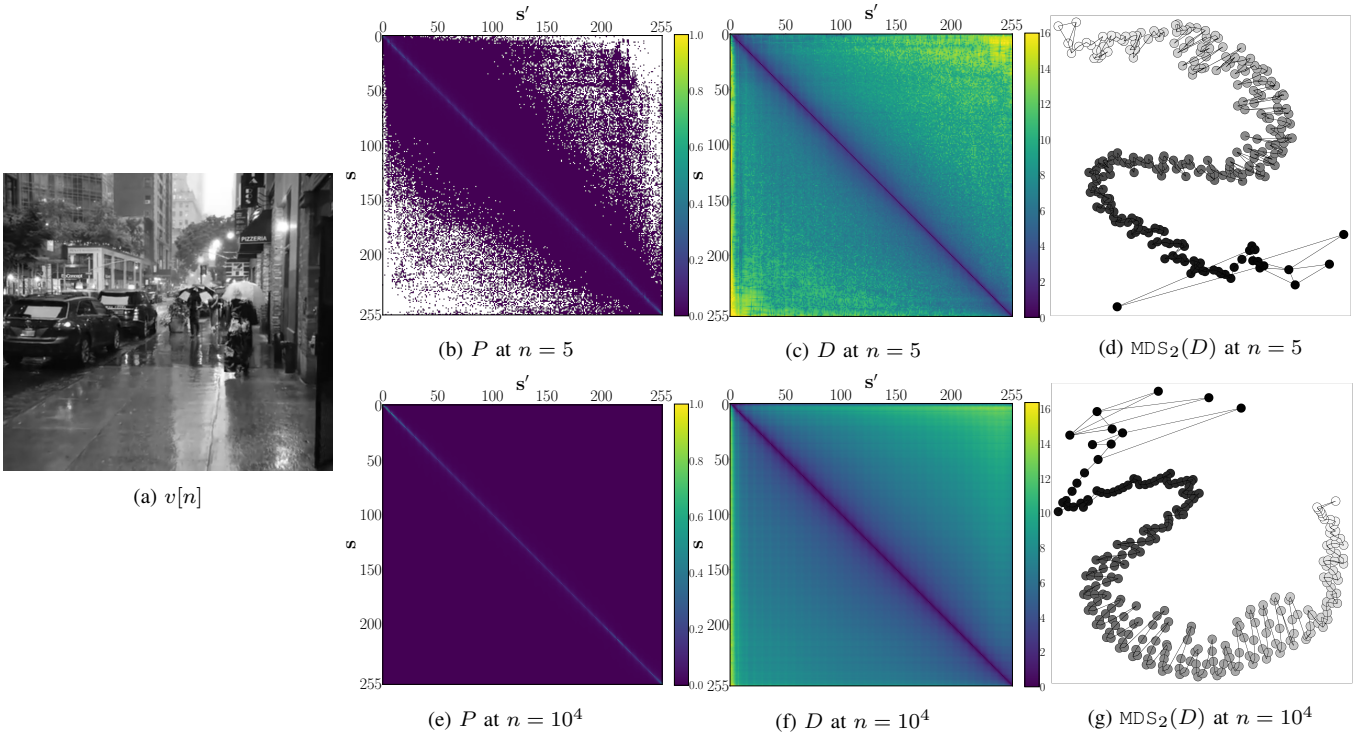

(a) $v[n]$ (b) P at $n = 5$ (c) D at $n = 5$ (d) $\texttt{MDS}_2(D)$ at $n = 5$

(e) P at $n = 10^4$ (f) D at $n = 10^4$ (g) $\texttt{MDS}_2(D)$ at $n = 10^4$

Figure 1: Building of the internal organization of sensory values. (a) Grayscale version of one frame of the video used in the experiment. (b)(e) Estimated probability matrix P at $n = 5$ and $n = 10^4$, i.e., at the very beginning of the experiment. (c)(f) Estimated distance matrix D at $n = 5$ and $n = 10^4$, i.e., at the end of the experiment. (d)(g) Corresponding low-dimensional embedding of D at $n = 5$ and $n = 10^4$: we can see the intuitive grayscale organization of pixel values, discovered by the agent from its sensory values transitions.

the experiment already exhibits a one dimensional manifold, with a thicker and less organized ordering of symbols. Again, the contribution of all sensels to the same statistic certainly explains this nice quick convergence of the representation. Thus, from the final graph, we can conclude that the agent has been able, starting only from the probability of transition between uninterpreted sensory symbols, to discover the gray level scale. Such a capability will be further exploited for different applications, like sensory prediction, see §V.

2) 2nd case: $h()$ is a sawtooth function: We will now consider a case where the agent's sensory output does not exactly match the original grayscale world as per Eq. (16), where $h() = \text{sawtooth}()$ is defined along

$$\text{sawtooth}(x) = \begin{cases} 2x & \text{if } 0 \leq x \leq 127 \\ 2(x - 128) & \text{otherwise,} \end{cases} \tag{17}$$

for $x \in [\![0; 255]\!]$ only. With such a change, a single internal sensory symbol (e.g., 54) will now correspond to two possible world grayscale values (27 and 155). Intuitively, such a change is expected to *create* continuity that does not exist initially between symbols through a closer proximity between values representing dark and light shades. The previous process is then repeated and the resulting 2D MDS embedding is depicted in Figure 2: as expected, we identify a looping monodimensional manifold. In the figure, each sensory symbol is depicted as a circle whose color represents its *internal* coding (i.e., a numerical value from 0 to 254 with a step of 2), represented as grayscale values for convenience. This color no longer matches the grayscale values of the world it represents because of the introduction of the sawtooth function. But the

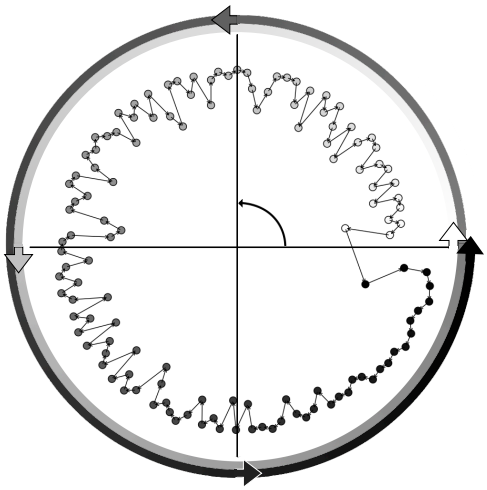

Figure 2: 2D MDS projection of the sensory symbols when a sawtooth function links together world gray values to sensory symbols. Each symbol is represented as a circle whose color represents the *internal* coding. The corresponding symbols *in the outside world* are represented as a looping arrow around the projection. *Internal* black (symbol 0) and white (symbol 255) symbols are now close to each other, differently from Figure 1g.

continuity initially captured in the previous experiment leads to a looping representation where the two opposite symbols, 0 and 254, are now close to each other in the internal representation as they both correspond to close grayscale values in the environment. Such a conclusion might be obvious in

this specific case, but it highlights that the *internal*, *subjective* representation of the sensory symbols' topology might actually differ greatly from our initial intuition as it depends on the way the agent's sensors encode sensory information. The same remark could apply to faulty sensors, whose output symbols could be modified or rearranged because of some failure in the information acquisition process; the proposed approach could then allow the agent to (re)build an adequate internal representation, though still intrinsically limited by its own defective sensory capabilities.

C. Results for color perception

To further illustrate the approach, we will now endow the agent with some color perception capabilities. Then, in this subsection, the initial color tuples $(R_{ij}, G_{ij}, B_{ij}) \in [\![0; 255]\!]^3$ coding the video pixel values v_{ij} are now mapped to the $\mathsf{S} = \alpha^3$ agent's sensels values $s_{ij} \in [\![0; \alpha^3 - 1]\!]$ along

$$s_{ij} = g(v_{ij}) = Q_\alpha(B_{ij}) + \alpha Q_\alpha(G_{ij}) + \alpha^2 Q_\alpha(R_{ij}), \quad (18)$$

with $Q_\alpha(.)$ a quantification function defined by

$$Q_\alpha : X \mapsto Q_\alpha(X) = \texttt{round}\left(\frac{X}{255} \times (\alpha - 1)\right), \quad (19)$$

with $X \in [\![0; 255]\!]$ and $Q_\alpha(X) \in [\![0; \alpha - 1]\!]$. Note that while the symbol ordering was quite obvious for grayscale values from an external point of view (e.g., the natural order from 0 to 255) for the various matrices M, P, Δ, and D, this no longer holds for these color sensory output symbols. Nevertheless, the order in which they appear as line or column indices in these matrices is not relevant since the only relevant information about their closeness is entirely independent of how these symbols are actually ordered. In all the following, $\alpha = 10$ is selected, so that the agent's sensory space is made of $\mathsf{S} = \alpha^3 = 1000$ uninterpreted (numerical) symbols. On this basis, all the previous steps are successively applied. The resulting D matrix can then be visualized through a low-dimensional embedding technique like ISOMAP [28]. The result of this projection performed in 3D is shown in Figure 3. The obtained representation is in line with some classical representations of RGB color models, like the HSL or HSV coding of color. Indeed, the 3D point cloud first appears to capture some color order very similar to the classical hue color wheel, where pure colors are represented through an angular position on a circle, as depicted in Figure 3a. But the 3D projection also exhibits a third axis linking very dark to very light shades for each color of the hue wheel, similar to the lightness axis in the HSV color coding, see Figure 3b. In order to assess in a more quantitative way the similarity of this low-dimensional projection with different color models, it is proposed to compute a Frobenius distance $\mathcal{F}$ along

$$\mathcal{F} = \| \, |D| - |D_m| \, \|, \quad (20)$$

where D_m is the $\mathsf{S} \times \mathsf{S}$ distance matrix between all the sensory symbols observed during the experiment for the color model $m \in \{\text{RAND, RGB, HSL, HSV}\}$, and $|.|$ the standardization operator. The resulting distances are reported in Table I, where the HSV color model better fits the obtained projection, as initially qualitatively intuited. The same study can be conducted by computing the k-nearest-neighbors between the obtained representation and the different color models. The result of such a study is also reported in Table I for $k = 75$ and exhibits the same conclusion. But one still has to keep in mind that finding the best fitting color model is not important by itself, since it is only exploited to *illustrate* the smooth transitions from one color symbol to another, without apparent discontinuity in the low dimensional embedding, as a way to represent the information actually captured by the agent in D, which is, in the end, the only data it exploits in the following. Then, with such a representation, the agent is now able to assess if the sensory symbol associated with the rose color is *closer* to the one associated with the red color than it is to the green one thanks to its internal metric matrix D.

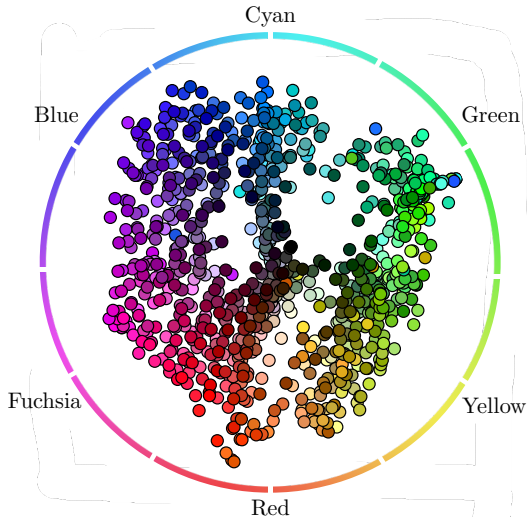

(a) 3D ISOMAP projection seen as a 2D color wheel.

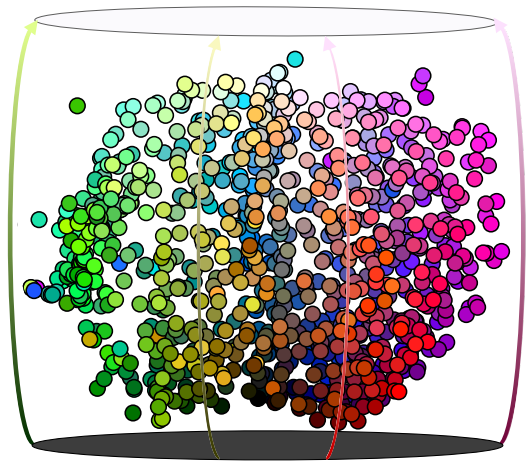

(b) The same 3D projection seen as a cylinder, with the lightness axis drawn as arrows from black to white.

Figure 3: Interpretation of the 3D ISOMAP projection of the matrix D when the agent is endowed with color perception capabilities. (a) Representation obtained when viewing the projection "from below": we can notice that all the sensory symbols are arranged by color, matching the intuitive color wheel which has been added to the graph. (b) Another point of view on the 3D sensory symbols representation: in addition to the color ordering highlighted in subfigure (a), a third axis supports the variation of lightness. The obtained projection can thus be understood as analogous to the HSL cylindre or biconic representation of the RGB color model.

Color model	RAND	RGB	HSL	HSV
Distance $\mathcal{F}$	1320	947	890.4	857.2
75-NN rate	8.4%	44.4%	45.5%	47.5%

Table I: Comparison between different color models, with RAND representing a random organization of the observed color symbols. (2nd line) Distances $\mathcal{F}$ between the low-dimensional projection and the corresponding color model. (3rd line) Rate of 75 nearest neighbors between the obtained representation and the corresponding color model.

IV. Locomotive motives: a case for fitting exploration and exploitation dynamics

The previous developments were largely devoted to the relationship between two internal observations: the transition probabilities and the resulting metric. We showed how this information allows the agent to build some notion of closeness between sensory symbols –which could be understood as some subjective notion of sensory continuity– from certain successions of sensory experiences being more likely, or *typical*, than others. But such considerations clearly rely on the idea that typical environment states also display certain typical patterns themselves. From an external point of view, one would certainly declare that "environment states are (mostly) continuous", both in time and space. This underlying assumption has not been dealt with so far, especially since the agent was passively observing sensory symbols changing over time in the previous experiments and not actively exploring its environment. This section thus aims to study which external structures in the states of the environment could explain the relationships between the agent's motor actions associated with a sensory experience and the observed regularity, effectively giving action a defining role in this internal assessment. We then propose to study the influence of the agent's action amplitude on its subjective sensory symbol continuity when it interacts with a mostly continuous environment. To that end, additional formal considerations are introduced in the first subsection. On this basis, some new experiments are proposed in the second subsection to highlight the importance of movement in building this subjective continuity.

A. Fitting spatial and sensory dynamics in the exploration

1) Spatial and temporal coherence: The results obtained in Section III were based on a purely passive observation of a changing "natural" visual scene –where the word *natural* here refers to our own usual and intuitive sensorimotor experience– allowing the agent to build a metric on its sensory symbols. But this distance should highly depend on the environment states and the successive configurations with which the agent samples it along time. More precisely, this implies that the environment's state should exhibit some typical patterns, both in space and time, in line with the manner in which the agent conducts its interaction, to make apparent the notion of certain sensory symbol transitions being "more typical" than others. Thus, one first condition to fulfill is *spatial*, mandating that e.g. immediately next to a red region $\mathcal{X}'$ of ambient space $\mathcal{X}$ it is more likely to be another region $\mathcal{X}''$ that is orange than cyan itself. In other words, we would generally expect the two events

$$\{\gamma_\epsilon(t)_{|\mathcal{X}'} = \epsilon_0\} \text{ and } \{\gamma_\epsilon(t)_{|\mathcal{X}''} = \epsilon_1\} \tag{21}$$

to largely depend on one another when $\mathcal{X}'$ and $\mathcal{X}''$ denote close (and small) regions of space. Furthermore, one second condition is *temporal*, so that the environment's state at any localization $\mathcal{X}'$ does not immediately change too randomly, so that the two events

$$\{\gamma_\epsilon(t)_{|\mathcal{X}'} = \epsilon_0\} \text{ and } \{\gamma_\epsilon(t+\Delta t)_{|\mathcal{X}'} = \epsilon_1\} \tag{22}$$

are conditioned on one another when Δt remains sufficiently small. We should insist on the fact that this coherence property, however, should only be local and relative to the agent's exploration dynamics. It is clear that the color of a point $x \in \mathcal{X}$ and time $t \in \mathscr{T}$ does not depend on which colors appear two kilometers away, one and a half days from there. On the other hand, should the agent instead perform a two-kilometers long movement between two successive time samples, it should not be able to infer any relationship between successive sensory readings from the sole spatial coherence constraints.

2) A formal account of spatiotemporal coherence: Let us now generalize the previous sensory transition probabilities (6) by introducing, for any (sub)collection of motor trajectories $\mathscr{B}'_{\mathscr{T}} \subseteq \mathscr{B}_{\mathscr{T}}$,

$$P^{\mathscr{B}'_{\mathscr{T}}}_{\mathbf{s}'|\mathbf{s}} = \{\gamma_{\mathbf{s}}(t+1) = \mathbf{s}' \mid \gamma_{\mathbf{s}}(t) = \mathbf{s} \text{ and } \gamma_{\mathbf{b}} \in \mathscr{B}'_{\mathscr{T}}\}, \tag{23}$$

for which $P^{\mathscr{B}'_{\mathscr{T}} = \mathscr{B}_{\mathscr{T}}}_{\mathbf{s}'|\mathbf{s}} = P_{\mathbf{s}'|\mathbf{s}}$. Such a (slight) generalization allows to highlight how a specific set of motor trajectories actually condition the sensory transitions available in the agent's sensorimotor flow. More precisely, we introduced in [16] the *sensor receptive field* as the specific region of space for which the state of the environment is sufficient to fully determine the agent's sensory state $\mathbf{s}$. Formally, a sensor receptive field can be seen as a function $F : \mathbf{b} \in \mathscr{B} \mapsto F(\mathbf{b}) \subset \mathcal{X}$ verifying

$$\begin{aligned} &\forall \epsilon_1, \epsilon_2 \in \mathcal{E}, \forall \mathbf{b} \in \mathscr{B}, \\ &\qquad \epsilon_{1|F(\mathbf{b})} = \epsilon_{2|F(\mathbf{b})} \Rightarrow \psi(\mathbf{b}, \epsilon_1) = \psi(\mathbf{b}, \epsilon_2) = \mathbf{s}. \end{aligned} \tag{24}$$

Then, let us now consider $\mathscr{B}'_{\mathscr{T}}$ as a set of motor explorations $\gamma_{\mathbf{b}}$ such that the receptive fields $F(\gamma_{\mathbf{b}}(t))$ and $F(\gamma_{\mathbf{b}}(t+1))$, which condition successive sensory outputs $\gamma_{\mathbf{s}}(t)$ and $\gamma_{\mathbf{s}}(t+1)$, fall *far apart* from one another. Then, based on our prior assumptions, the corresponding local environment states $\gamma_{\epsilon|F(\gamma_{\mathbf{b}}(t+1))}(t+1)$ and $\gamma_{\epsilon|F(\gamma_{\mathbf{b}}(t))}(t)$ should be independent: the physical properties available to the agent in the environment, restricted to the regions of space it would sample at time t and $t+1$ by following a motor trajectory $\gamma_{\mathbf{b}} \in \mathscr{B}'_{\mathscr{T}}$, should not depend on each other. It then follows that $\gamma_{\mathbf{s}}(t+1) = \gamma_{\gamma_{\mathbf{b}}(t+1), \epsilon|F(\gamma_{\mathbf{b}}(t+1))}(t+1)$ and $\gamma_{\mathbf{s}}(t) = \gamma_{\gamma_{\mathbf{b}}(t), \epsilon|F(\gamma_{\mathbf{b}}(t))}(t)$ should be independent themselves. As a result, we have

$$\begin{aligned} P^{\mathscr{B}'_{\mathscr{T}}}_{\mathbf{s}'|\mathbf{s}} &= \{\gamma_{\mathbf{s}}(t+1) = \mathbf{s}' \mid \gamma_{\mathbf{s}}(t) = \mathbf{s}, \gamma_{\mathbf{b}} \in \mathscr{B}'_{\mathscr{T}}\}, \\ &= \{\gamma_{\mathbf{s}}(t+1) = \mathbf{s}' \mid \gamma_{\mathbf{b}} \in \mathscr{B}'_{\mathscr{T}}\}. \end{aligned} \tag{25}$$

Thus, the probability $P^{\mathscr{B}'_{\mathscr{T}}}_{\mathbf{s}'|\mathbf{s}}$ –where $\mathscr{B}'_{\mathscr{T}}$ is a motor trajectory for which the coherence properties mentioned before are not verified– should not depend on previous sensory output $\mathbf{s}$ anymore; instead, it simply replicates the *un*conditional probability that the agent experiences the particular sensory value $\mathbf{s}$'. To the agent, this means that the knowledge of which sensation $\mathbf{s}$ it experiences at timestep t does not give it *any* information on which sensation $\mathbf{s}'$ it is poised to experience at

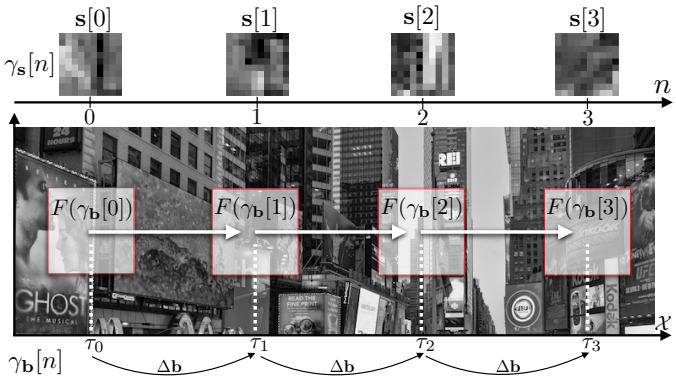

Figure 4: Experimental setup to assess the effect of the agent's movement on the internal sensory symbol topology. A camera, whose field of view –or receptive field– is drawn as a square with red borders, faces a grayscale image and moves from one position τ to another thanks to an action of amplitude $\Delta\mathbf{b}$. The corresponding sensory states $\mathbf{s}[n]$ are then captured along time to build the statistics of the sensory symbol transitions.

$t+1$. Importantly, this shows that suitable choices of motor explorations are required for building a valid sensory metric, as well as giving an internal observation to assess whether this condition fails through Equation (25). The influence of this motor exploration is experimentally studied in the next subsection to illustrate these developments.

B. An experimental assessment of the influence of the movement amplitude

We propose in this subsection to assess the effect movement of the agent has on the internal representation of sensory symbols through simple simulations, where the agent is now allowed to move in a fixed environment. To begin with, details about the experiment setup are given. Next, the resulting representations are analyzed and discussed.

1) Experimental setup: let us consider in all the following a very simple agent, whose body is made of a planar, rectangular, camera sat atop one actuator, allowing the agent to only move in one direction, see Figure 4. The pixels of the camera are sensitive to the luminance of the ambient stimulus, which is a fixed grayscale image placed in front of the moving camera. In such a case, the ambient space $\mathcal{X}$ is then the plane $\mathbb{R}^2$, and the state of the environment is a function ϵ mapping a position (x, y) in the plane to luminance values $\epsilon(x, y) \in [\![0; 255]\!]$ as encoded in the grayscale image. Those values are then converted into a sensory vector $\mathbf{s} \in [\![0; 255]\!]^{W \times H}$ directly capturing the corresponding grayscale value in the environment (the function $h()$ in Equation (16) is thus the identity function). In the forthcoming simulations, $W = H = 100$. As already outlined in §II-A, we consider the agent is able to move in its environment by applying a single *action* a [16], i.e. by applying a function a to its current absolute configuration $\mathbf{b} = (\mathbf{m}, \tau)$ to go to another configuration $\mathbf{b}' = (\mathbf{m}', \tau') = a\mathbf{b}$. In this section, we will mainly study the influence of the amplitude $\Delta\mathbf{b}$ of this action, which is supposed to produce a movement of the camera in only one direction and with the same amplitude, as illustrated in Figure 4. This is obviously a very particular and restrictive action, at least in comparison with the more generic motor action framework presented by the authors in [16], but it will still allow a comprehensive study of the effect of movement on the internal representation built by the agent. The different action amplitudes $\Delta\mathbf{b}$ used in the simulations will all be equal to a multiple of $\sigma_{\mathbf{b}}$, a particular amplitude which causes a shift of the perceived information in $\mathbf{s}$ of exactly 1 pixel. This actually corresponds to a displacement of the camera receptive field $F(\mathbf{b})$ in $\mathcal{X}$ (represented as squares with red borders in Figure 4) of the width of 1 pixel in the plane supporting the grayscale image. Note that the amplitude of the actions is explicitly an *external* metric that is not available to the agent; all it knows about is that it is using an action with an unknown amplitude to move in its environment. We will show in §IV-B3 that, under the proposed assumptions, the agent will be able to compare the amplitude of its actions on the basis on their sensory consequences.

In practice, the experiment is conducted the following way: to begin with, the environment observed by the agent is a grayscale image of a crowded street, partially shown in Figure 4. Then, starting from a fixed (random) position τ_0 in the environment, the agent follows a motor trajectory $\gamma_{\mathbf{b}}[n]$ made of jumps of fixed amplitude $\Delta\mathbf{b}$. This produces a displacement of the agent's sensor receptive field in the environment at which the agent gathers samples $\mathbf{s}[n]$ of its corresponding sensory trajectory $\gamma_{\mathbf{s}}[n]$. After having generated N_a times the same action a, the camera is put in one other random position in the image; then, the action a is used again to move the camera N_a times in the image. This process is repeated N_r times, so that $N_r \times N_a$ sensory samples $\mathbf{s}[n]$ are collected. These samples then allow one to build the matrix P as in Equation (13). Then, the corresponding MDS projection of the distance matrix D can be computed to visualize the captured sensory symbol topology. The experience is finally repeated for various amplitudes $\Delta\mathbf{b}$.

2) Results: The experiment has been conducted for $N_a = 500$ and $N_r = 100$, so that 50.10^3 sensory transitions are used to build the matrix P for each action amplitude $\Delta\mathbf{b}$ chosen among $\{\sigma_{\mathbf{b}}, 25\sigma_{\mathbf{b}}, 250\sigma_{\mathbf{b}}, 1000\sigma_{\mathbf{b}}\}$. Note that being greater than the size $N_s = 100$ of the sensor, $\Delta\mathbf{b} = 250\sigma_{\mathbf{b}}$ leads to the sampling of an area in the environment that does not overlap with its previous receptive field position. Figure 5 represents successively (in each row) the matrices P, D and their corresponding embedding $\mathtt{MDS}_2(D)$ for each of the 4 selected amplitudes (in each column). Let us first consider the evolution of the probability matrix as a function of the movement amplitude (first row). For a very small action amplitude, the probability matrix P exhibits a clear diagonal pattern indicating that close sensory symbols (in terms of gray levels) correspond to high transition probabilities; qualitatively, we face more or less the same conditions than in §III-B1 where the observation of the environment changes matches the changes in perception induced by the action of the agent. These two scenarios no longer correspond when the action amplitude rises: the higher the amplitude, the wider the probability distribution. For the largest amplitude, the diagonal pattern cannot even be seen anymore in P and high probabilities do not correspond to close gray levels anymore. This tendency is clearly confirmed when computing the distance matrix D from P (2nd row in Figure 5): for high amplitudes, mostly all

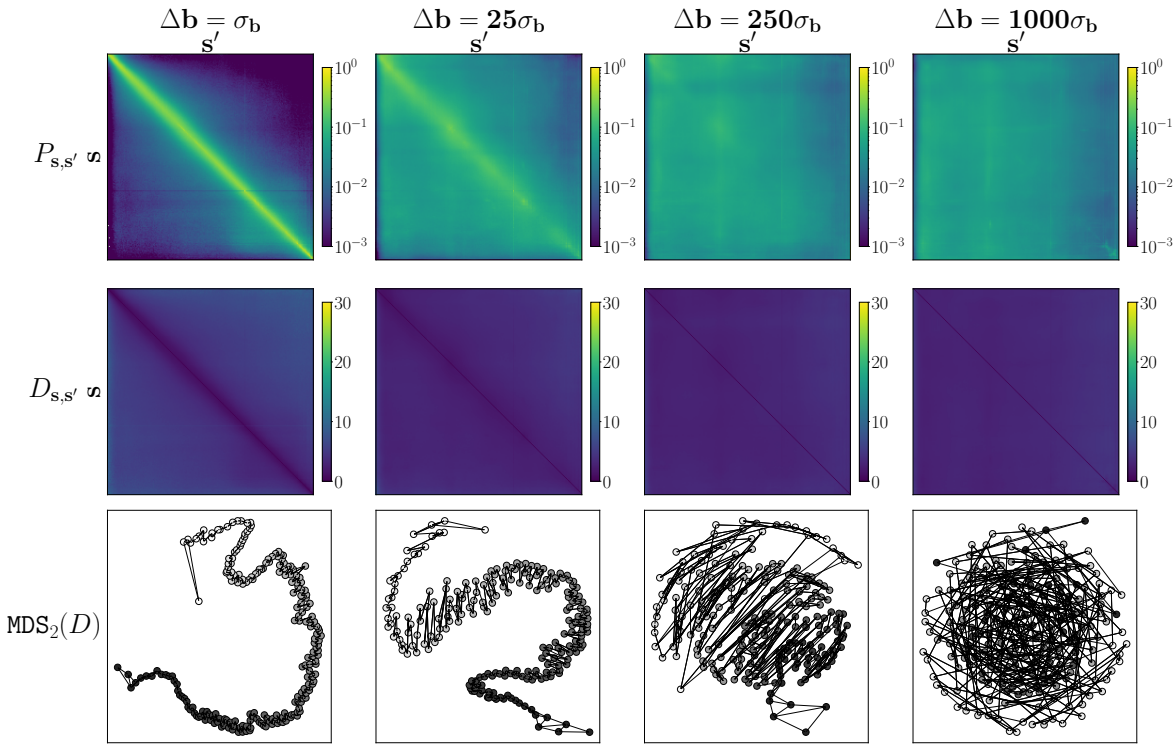

Figure 5: Evolution of the transition probability measure P (displayed with a logarithmic norm), the distance measure D and the representation of this distance projected using 2-dimensional MDS for increasing movement amplitudes. Each column represents a motor trajectory for a fixed amplitude $\Delta\mathbf{b}$ described relative to a 1 pixel shift of its sensor's field of view. We can see that the diagonal pattern for P and D as well as the uni-dimensional grayscale manifold are deteriorating as the movement amplitude gets bigger, indicating the inability to capture spatial coherence properties. The links that connect each symbol on the MDS representation are a k-NN like algorithm that assess how the agent perceive its symbol continuity.

symbols are now close to each other. Obviously, this results in very different $2D$ projections of the matrix D (3rd row). For the lowest amplitudes, we still clearly see a one-dimensional manifold, folding on itself when the action amplitude grows. But the dimensionality of the manifold is not sufficient to tell if the agent correctly captured or not the sensory symbol topology. Like we did in Figure 1g and Figure 1d, a k-NN algorithm is computed on D and displayed in Figure 5 to link each symbol to its closest neighbor, this link being represented as a line between two symbols in the projection. Looking at the smallest amplitude, the sensory symbols manifold can be browsed in the usual grayscale order by following the aforementioned lines. On the contrary, this proves impossible for larger amplitudes, where lines link together e.g., symbols associated with clear and dark gray levels. It is then clear that the conditions written as Equations (21) and (22) are not verified anymore, with two successively sampled environment states associated with two distant positions in space, leading to the loss of perception by the agent of the spatial and temporal coherence in the environment.

3) Discussions: Equation (25) states that, for a specific set of motor trajectories $\mathscr{B}'_{\mathscr{T}}$ making successive receptive fields falling apart from one another, the probability of transition between successive sensory symbols tends to an *un*conditional probability $P^{\mathscr{B}'_{\mathscr{T}}}_{\mathbf{s}'|\mathbf{s}} = P_{\mathbf{s}'}$. Importantly, this phenomenon can be *internally* assessed by the agent since both probability distributions are only based on sensory symbol observations; this then constitutes some *internal* way for the agent to rate the spatial and temporal coherence of its interaction with the environment. To that end, we propose to compare the two probability distributions $P_{\mathbf{s}'|\mathbf{s}=\mathbf{s}_k}$ –the probability of every sensory value to succeed to a specific sensory value $\mathbf{s}_k$– and $P_{\mathbf{s}'}$, by using the Jensen-Shannon distance D_{JS} [29], a bounded metric based on the symmetrized version of the Kullback–Leibler divergence [30], and defined as

$$D_{\text{JS}}(P_{\mathbf{s}'|\mathbf{s}=\mathbf{s}_k} \| P_{\mathbf{s}'}) = \sqrt{\frac{\text{KL}(P_{\mathbf{s}'|\mathbf{s}=\mathbf{s}_k} \| M) + \text{KL}(P_{\mathbf{s}'} \| M)}{2}},$$
$$\text{with } M = \frac{1}{2}\left(P_{\mathbf{s}'|\mathbf{s}=\mathbf{s}_k} + P_{\mathbf{s}'}\right), \tag{26}$$

with the KL divergence for two discrete probabilistic distributions A and B defined in the probability space $\mathcal{W}$ as

$$\text{KL}(A \| B) = \sum_{x \in \mathcal{W}} A(x) \log_2 \left(\frac{A(x)}{B(x)}\right). \tag{27}$$

This results in a distance $D_{\text{JS}}(.)$ between 0 and 1, computed for each sensory symbol $\mathbf{s}'$, that is expected to converge towards 0 when both distributions are identical, i.e. when the motor trajectory of the agent leads to having $\mathbf{s}$ and $\mathbf{s}'$ independent. Again, D_{JS} is computed for 4 different amplitudes $\{\sigma_\mathbf{b}, 5\sigma_\mathbf{b}, 25\sigma_\mathbf{b}, 125\sigma_\mathbf{b}\}$ with corresponding graphs in Figure 6. The results displayed in Figure 6 show that the JS distance for every probability distribution systematically decreases when the amplitude of the agent's movement increases, i.e. when

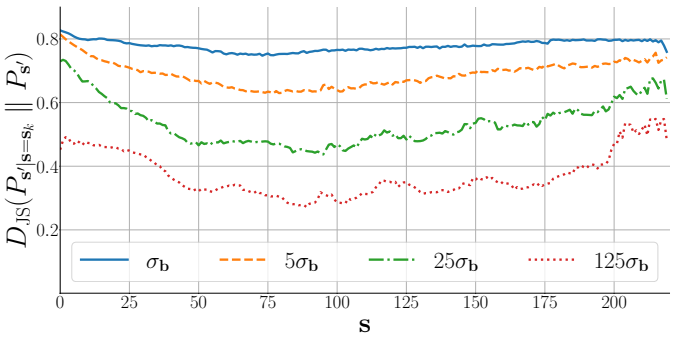

Figure 6: JS distance of every conditional probabilities relatively to the unconditional probability $P(\mathbf{s}')$ for different movement amplitudes. Each point of the plot represents a JS distance for a single conditional probability to $P(\mathbf{s}')$. As the amplitude increases, the divergence of every symbol decreases, getting close to the unconditional probability.

$\Delta\mathbf{b}$	$\sigma_{\mathbf{b}}$	$5\ \sigma_{\mathbf{b}}$	$25\ \sigma_{\mathbf{b}}$	$125\ \sigma_{\mathbf{b}}$
$I(\mathbf{s},\mathbf{s}')$	5.36	3.49	1.92	0.94

Table II: Mutual information between sensory symbols $\mathbf{s}$ and $\mathbf{s}'$ as a function of the agent's action amplitude.

the conditional distribution tends towards the unconditional one as described by Eq. (25). In the same vein, we can also conduct this comparison by computing the mutual information between, roughly speaking, the sensory symbols before and after the agent's movement and defined by

$$I(\mathbf{s},\mathbf{s}') = \sum_{k,l} p_{\mathbf{s}_k,\mathbf{s}_l} \log_2 \left(\frac{p_{\mathbf{s}_k,\mathbf{s}_l}}{p_{\mathbf{s}_k} p_{\mathbf{s}_l}} \right), \tag{28}$$

with $P_{\mathbf{s},\mathbf{s}'} = (p_{\mathbf{s}_k,\mathbf{s}_l})_{\mathbf{s}_k,\mathbf{s}_l}$ the joint probability and $P_{\mathbf{s}} = (p_{\mathbf{s}_k})_{\mathbf{s}_k}$ and $P_{\mathbf{s}'} = (p_{\mathbf{s}_l})_{\mathbf{s}_l}$ the marginal probabilities. This mutual information is computed for the same 4 amplitudes as in Figure 6, and is reported in Table II. As expected, the mutual information drops significantly by about 64% as soon as the movement amplitude rises to $25\sigma_{\mathbf{b}}$, showing again how the link between $\mathbf{s}$ and $\mathbf{s}'$ is degraded when the agent's motion amplitude becomes higher between two time steps. Importantly, these two comparisons between the two probability distributions could provide the agent with an *internal* way to rate the adequation of its motor exploration performed by applying actions with (at least for now) unknown consequences, or even an internal signature of the amplitude of its own actions.

V. Using the metric to get an internal assessment of sensory regularity

Now that we have been able to quantify how and why the agent's action modulates its sensory symbol topology, let us focus on a more experimental use of the obtained representation. Intuitively, and thanks to the introduction of the metric d_f, the agent should now be able to assess if a sensory transition is typical or not. This could be used as a way to deal with the presence of noise in the raw sensory data, i.e. by being able to discriminate close (but not strictly equal) sensory values from irregular sensory transitions due to the presence of specific events in the environment (movement of an object in the scene, changes in the illumination conditions, etc.). This section thus aims to present how the agent could internally assess its sensory regularity by first depicting some simple formal elements in the first subsection. Then, the second subsection shows how a naive agent could actually be capable of performing a sensory prediction task, even in the presence of noise, in the vein of the sensorimotor action framework presented by the authors in [16].

A. Internally rating the sensory regularity

1) Some formal considerations: to begin with, let us consider again Eq. (7) by which $\delta_f(\mathbf{s},\mathbf{s}')$ is defined in terms of the sensory transition probabilities $P_{\mathbf{s}'|\mathbf{s}}$. It can be trivially rewritten as

$$\forall \mathbf{s},\mathbf{s}' \in \mathcal{S}, \mathbb{P}(\gamma_{\mathbf{s}}(t+1) = \mathbf{s}' \mid \gamma_{\mathbf{s}}(t) = \mathbf{s}) = f^{-1}(\delta_f(\mathbf{s},\mathbf{s}')), \tag{29}$$

when f is injective. But because f is also necessarily non-increasing, so must be f^{-1}; this obviously entails that the probability of any sensory transition from $\mathbf{s}$ to $\mathbf{s}'$ is as expected a decreasing function of the sensory distance between them. However, we also know from the definition of the metric d_f from shortest paths in Eq. (9) that

$$\forall \mathbf{s},\mathbf{s}' \in \mathcal{S}, \mathrm{d}_f(\mathbf{s},\mathbf{s}') \leq \delta_f(\mathbf{s},\mathbf{s}'). \tag{30}$$

We then have immediately

$$\forall \mathbf{s},\mathbf{s}' \in \mathcal{S}, \mathbb{P}(\gamma_{\mathbf{s}}(t+1) = \mathbf{s}' \mid \gamma_{\mathbf{s}}(t) = \mathbf{s}) \leq f^{-1}(\mathrm{d}_f(\mathbf{s},\mathbf{s}')). \tag{31}$$

Then, Eq. (31) guarantees that, from any sensory value $\mathbf{s}$, the probability to land on $\mathbf{s}'$ at a distance $\mathrm{d}_f(\mathbf{s},\mathbf{s}') = \lambda$ is therefore *less than* $f^{-1}(\lambda)$. This property thus gives an intrinsic way of quantifying the *regularity* of a transition in the sensory experience. Indeed, providing some "metric rejection threshold" τ_r, the agent might be able to deem all sensory transitions $\mathbf{s}$ to $\mathbf{s}'$ of corresponding distance $\mathrm{d}_f(\mathbf{s},\mathbf{s}')$ as irregular (resp. regular) whenever $\mathrm{d}_f(\mathbf{s},\mathbf{s}') \geq \tau_r$ (resp. $\mathrm{d}_f(\mathbf{s},\mathbf{s}') < \tau_r$). Obviously, determining whether a transition is regular or not might also be decided directly on the basis of its probability of transition. To stay consistent, we choose to only investigate the properties of our regularity measure from the standpoint of the sensory metric.

Still, one should notice that Eq. (31) is merely an inequality, as opposed to the corresponding equality in Eq. (29). To the agent, this means that there may be some particular transitions from $\mathbf{s}$ to $\mathbf{s}'$ which are still unlikely even if the agent found $\mathrm{d}_f(\mathbf{s},\mathbf{s}')$ to be small: basically, this criterion can allow *false positives*, while it guarantees that all transitions rejected on the basis of this metric verify the occurrence probability inequality, that is it does not cause *false negatives*.

2) Example: we selected in previous sections (see Eq. (14)) the function $f = -\log$ to map the estimated transition probabilities p_{kl} to the metric prototype δ_{kl}. In such a case, still with a threshold τ_r, an irregular transition should then typically occur with a probability $\mathbb{P}(\gamma_{\mathbf{s}}(t+1) = \mathbf{s}' \mid \gamma_{\mathbf{s}}(t) = \mathbf{s}) \leq e^{-\tau_r}$. Then, selecting for instance the threshold values $\tau_r \in \{1,3,5\}$ will allow the agent to reject transitions that occur in less than about $\{37,5,1\}$% of occurrences.

B. Exploiting the sensory regularity for sensory prediction

We now propose to exploit the agent's capability to decide whether a sensory transition is regular in a sensory prediction task in the presence of noise inside the sensory data. To that end, the framing of the approach in [16] is first briefly introduced, followed by the proposed experimental setup, mirroring that of this previous contribution. Then, the sensory prediction framework from [16] is applied for different scenarios: (i) with no noise in the sensory data or with noise, but (ii) without or (iii) with rating the sensory regularity. A discussion comparing these scenarios is then proposed in the second paragraph.

1) A short recall on the framing of the problem: The contribution from [16] is all about the theoretical conditions for the determination of a sensory prediction function for a naive agent. More precisely, it is demonstrated how the algebraic structure found in this prediction is homeomorphic to that of an algebraic group of specific motor actions, the *conservative* actions. An action a is said to be conservative if all sensels of the agent exchange the places they sample when applying a: equivalently, conservative actions can then be thought of as permutations of sensels. Importantly, this result has since been extended to *quasiconservative* actions in [23], where partial sensory prediction maps are proposed to generalize the sensel permutations of strictly conservative actions for the case where some sensels have no identified permutations when applying an action a (e.g. for sensels in the border of a camera).

2) Experimental setup: the proposed simulation setup is very close to the one already presented in §IV-B1. The agent is still made of a moving camera facing a fixed grayscale image, as shown in Figure 4. This time, the agent is endowed with a $W \times H = 10 \times 10$ sensor, and is now able to move in four orthogonal directions by applying 5 different (quasiconservative) actions: a_{id}, a_f, a_b, a_r and a_l making the camera receptive field respectively stay still, move in the left, right, up or down directions in $\mathcal{X}$. It is clear that the sensory consequences of such actions can be illustrated as a shift of information in the image in the opposite direction of the agent's movement: most of the sensels values *before* applying any of these actions can find a successor *after*. Then, predicting the sensory consequence of an action can be summed up by a permutation between sensel values, providing all sensels share the same excitation function, as already outlined in §III-A2. Importantly, the agent has no clue about the incidence of a given action nor about their possible relationship. All it can do is perform an action and observe its consequences in its sensory data [16]. The proposed experimentation then relies on the two following steps.

a) Step 1: building of the sensory symbol topology. The agent explores its environment by repeatedly selecting random actions in $\mathcal{A} = \{a_{\text{id}}, a_f, a_b, a_r, a_l\}$ with identical amplitudes $\Delta\mathbf{b} = \sigma_{\mathbf{b}}$ (apart from a_{id}), and then infers the distance matrix D, in line with §IV-B where the number N_a of draws of actions is set to $N_a = 25$, and the number of repetition is selected to $N_r = 2.10^3$. As opposed to the previous case, some artificial noise n_{ij} is now added to the pixel value v_{ij} of the image to form the agent's sensel values[3] $s_{ij} = v_{ij} + n_{ij}$ before computing the matrix D, with n_{ij} a random integer drawn from a centered discrete uniform distribution of width $2\sigma_n$.

b) Step 2: building of the sensory prediction function. Once the matrix D is obtained, the agent performs a second exploration of its environment so as to build a sensory prediction function for each of its actions in $\mathcal{A}$. As previously argued, these functions can take the form of binary permutation matrices [16] $\Pi_{a_p} = (\pi_{kl}^{(p)})_{k,l}$ of size $N_s \times N_s$, with $a_p \in \mathcal{A}$ and $N_s = W \times H$, as each pixel value in the sensory array is expected to shift in different positions depending on the spatial effect of the performed action. In these matrices, having $\pi_{kl}^{(p)} = 1$ indicates that the kth sensel takes the value of the lth sensel after applying action a_p. For this experiment, $N_a = 50.10^3$ and $N_r = 1$. Initially, every element $\pi_{kl}^{(p)}$ of the permutation matrices Π_{a_p} is initialized to 1, meaning that all permutations between the agent's sensels are possible for action a_p. Then, each time this action is drawn from $\mathcal{A}$, the agent can discard in Π_{a_p} some permutations by observing that some sensel values do not switch with one another, then updating the corresponding matrix elements to 0 as per the update rule

$$\pi_{kl}^{(p)}[n+1] = \begin{cases} 1 \text{ iff } s_l[n] = s_k[n+1] \text{ and } \pi_{kl}^{(p)}[n] = 1 \\ 0 \text{ else,} \end{cases} \quad (32)$$

where s_k and s_l represent the sensel values associated with the element at the position (k, l) in the permutation matrix Π_{a_p}. We can notice in Eq. (32) that the elements in these matrices are set to 0 as soon as a permutation is not detected by the strict equality between sensory values. This limitation, already outlined in [16], makes this approach fall apart when dealing with noise in the sensory data or when interacting with a non-static environment. Benefiting from the previous developments, we instead propose a revised update rule for the permutation matrix as

$$\pi_{kl}^{(p)}[n+1] = \begin{cases} 1 \text{ iff } \mathrm{d}_f(s_l[n], s_k[n+1]) < \tau_r \text{ and } \pi_{kl}^{(p)}[n] = 1 \\ 0 \text{ else,} \end{cases} \quad (33)$$

where τ_r is a manually chosen threshold applied to the built matrix distance D. In the following, τ_r is tuned so as to correspond to the smallest threshold that allows for permutation matrices to converge. It is clear that this is a strong *a priori*, and the way the agent can autonomously set this threshold is still an ongoing work, discussed in the conclusion. In the same vein, the second step in this experiment requires a second exploration of the *same* environment as during the first step. This definitely a suboptimal process, only proposed here to illustrate the benefits of the internal assessment of sensory regularities for the proposed sensory prediction task. Obviously, the sensory transitions observed when building the sensory symbol topology could also be used for building the sensory prediction functions. Importantly, this highlights again the importance of the threshold τ_r which should then also be selected by an appropriate combination of these two steps.

c) Evaluation: convergence of the permutation matrices. To evaluate the influence of the added noise on the convergence of permutation matrices Π_{a_p}, we propose an (external) criterion $C(\Pi_{a_p}) = C_H(\Pi_{a_p}) \times C_D(\Pi_{a_p})$ adapted from [16]

[3] which is further clamped if need be, i.e. if s_{ij} exceeds 0 or 255, the sensel value is set to the closer bound.

to account for the added noise to the data and defined along

$$C_D(\Pi_{a_p}) = \frac{\sum_{kl} \pi_{kl}^{(p)} \bar{\pi}_{kl}^{(p)}}{\sum_{kl} \bar{\pi}_{kl}^{(p)}}, \text{ and}$$
$$C_H(\Pi_{a_p}) = 1 - \frac{1}{N_s \log_2(N_s)} \sum_{i=1}^{N_s} H_i, \tag{34}$$

with

$$\begin{cases} H_i &= -\sum_{l=1}^{N_s} \frac{\pi_{kl}^{(p)}}{\mu_k} \log_2\left(\frac{\pi_{kl}^{(p)}}{\mu_k}\right), \\ \mu_k &= \max\left(1, \sum_{l=1}^{N_s} \pi_{kl}^{(p)}\right), \end{cases} \tag{35}$$

where $\bar{\pi}_{kl}^{(p)}$ represents the (binary) coefficients of the ideal matrix $\bar{\Pi}_{a_p}$ associated with the action a_p. Basically, C_H can be understood as an average measure of certainty in the discovery of the permutations, weighted by the percentage C_D of the correctly identified permutations w.r.t. the ground truth to account for the noise, possibly discarding some of them. In the end, criterion C lies between 0 –i.e. the matrix is full of 1's (initialization) or 0's (all permutations have been discarded)– and 1 –i.e. the permutation has been correctly discovered.

3) Results: As outlined in the introduction of Section V, three different scenarios are evaluated. To begin with, we first consider the case where there is no noise in the agent's perception by setting $\sigma_n = 0$. Then, using the update rule (32) should allow the agent to correctly build all of its permutation matrices, exactly as in in [16]. As expected, Figure 7a shows that criterion C converges towards its maximal value of 1 for all actions in $\mathcal{A}$. C plots also exhibit sparse jumps at random times, corresponding to the steps where the action was actually drawn in $\mathcal{A}$ during the experiment. More importantly, we can see in Figure 7a that only a few realizations of each action a_p (about 4 to 6 here) are required for $C(\Pi_{a_p})$ to almost reach 1, showing how easy it is for the agent to discover the existence of such permutations in its own perception. In the second scenario, a noise of amplitude $\sigma_n = 2$ is now added to the sensation. Obviously, the strict comparison of sensel values in (32) in the presence of such noise (however small) entirely breaks the approach , as shown in Figure 7b. As expected, the criterion C now converges to 0: each Π_{a_p} matrices converges to null matrices as all possible permutations of values have been (including erroneously) discarded in the process. Finally, the new update rule (33) is now used to judge the closeness of sensel values on the basis of the built distance D, resulting in the evolution of the criterion C represented in Figure 7c. For this scenario, $\sigma_b = 1$ and $\tau_r = 1.63$. In the presence of noise, the ability of the agent to assess if a sensation is now close to others allows it to correctly discover the existence of permutations in its perception. But clearly, this task is not as easy as in the first scenario: the number of required actions for correctly evaluating their corresponding permutation matrices is significantly higher. This is apparent in Figure 7c, not only in the slower convergence time of the criterion C but also in the smaller jumps of values in C. Indeed, each generation of action brings less information in the prediction process because of the noise included in the agent's sensations. But still, the important structures anchoring the sensorimotor interaction the agent has with its environment are still available, allowing it e.g., to build an image of its body [14] or of its peripersonal space [15], at least at the cost of a longer interaction in time.

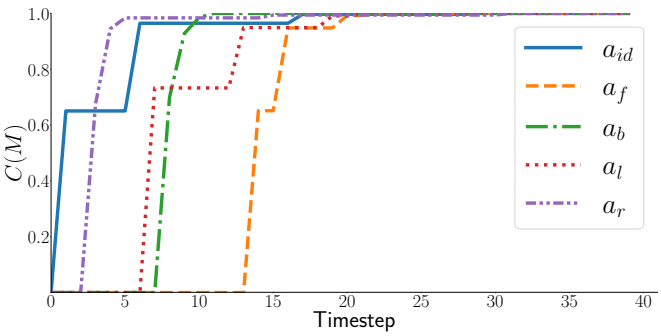

(a) Evaluation criterion C with $\sigma_n = 0$ and strict equality update rule.

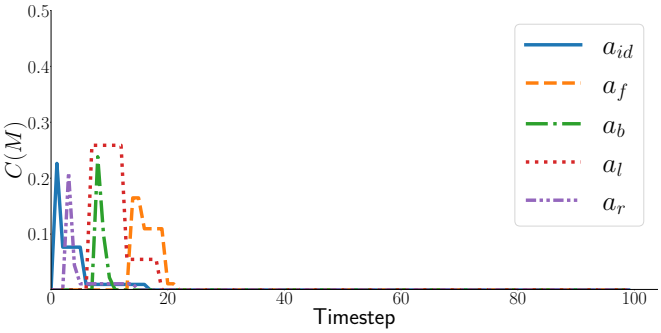

(b) Evaluation criterion C with $\sigma_n = 2$ and strict equality update rule.

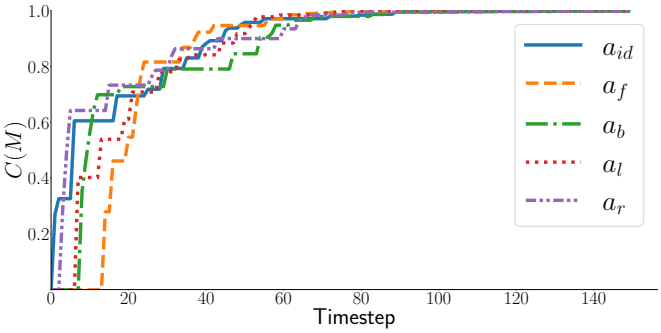

(c) Evaluation criterion C with $\sigma_n = 2$ and a threshold in D.

Figure 7: Evolution of the evaluation criterion C for the 5 considered actions in $\mathcal{A}$. (a) With no noise and the update rule (32), C converges towards 1 in a very short number of realizations of each action. (b) In the same scenario, but with $\sigma_n = 2$, the update rule (32) do not allow to detect permutations anymore, resulting in the criterion falling down to 0. (c) When selecting a correct threshold τ_r in Eq. (33), the agent is now able to build the 5 sensory prediction functions correctly, but with more realization of each action in comparison with (a).

VI. Conclusion

In this paper, and after purely topological considerations, a metric-based approach is proposed to formalize the ability of a naive agent to build some subjective sense of sensory continuity. An experimental framework is then proposed, illustrated and assessed in the context of visual perception for the discovery of gray or color scales. Then the importance of the dynamic of the agent's exploration relative to that of the environment is studied, highlighting an important spatiotemporal coherence principle of this exploration. Finally, with a sensory closeness notion now available to the agent, a sensory

prediction task is proved accessible even in the presence of noise, thus extending the robustness of this sensorimotor framework to realistic conditions.

Nevertheless, it is clear that this work still suffers from some limitations. For instance, the scalability of the proposed experimental framework is certainly limited. Indeed, although it was not the objective of this paper, the way the regularities are extracted from the raw sensations is certainly not computationally effective, considering the possibly very high number of sensory symbols involved in e.g., color perception for traditional camera sensors. Hierarchical approaches might be preferred [31], but still remain to be explored in the context of sensorimotor approaches to perception. Another limit concerns the notion of sensory neighbors: while being now formally accessible to the agent thanks to the proposed contribution, it still practically requires a threshold to be set w.r.t. the task to be performed. In this paper, this threshold has been manually tuned with two successive steps involving two independent explorations of the same environment, but we could instead rely on a closed-loop approach mixing the discovery of the sensory regularities with the corresponding sensory prediction task: as long as the prediction is not correctly built, the threshold must be adapted accordingly. Still, should the agent be able to perform some sensory prediction task, so should it be able to *quantitatively* compare its prediction with its actual perception. This should make it capable of detecting outliers in its environment, and in particular, changes in its perception that are not directly correlated to its own actions. This might be the way towards some internal notion of sensorimotor objects and thus would undoubtedly extend the scope of these approaches to more potential applications.

References

[1] B. Dainton, "Temporal Consciousness," in *The Stanford Encyclopedia of Philosophy*, Winter 2018 ed., E. N. Zalta, Ed. Metaphysics Research Lab, Stanford University, 2018.

[2] J. M. B. Fugate, "Categorical perception for emotional faces," *Emotion Review*, vol. 5, no. 1, pp. 84–89, 2013.

[3] J. C. Toscano, B. McMurray, J. Dennhardt, and S. J. Luck, "Continuous perception and graded categorization: Electrophysiological evidence for a linear relationship between the acoustic signal and perceptual encoding of speech," *Psychological Science*, vol. 21, no. 10, pp. 1532–1540, 2010.

[4] A. Herwig, "Transsaccadic integration and perceptual continuity," *Journal of Vision*, vol. 15, no. 16, pp. 7–7, 12 2015.

[5] J. M. Stroud, "The fine structure of psychological time," *Annals of the New York Academy of Sciences*, vol. 138, no. 2, pp. 623–631, 1967.

[6] R. VanRullen and C. Koch, "Is perception discrete or continuous?" *Trends in Cognitive Sciences*, vol. 7, no. 5, pp. 207–213, 2003.

[7] J. O'Regan, *Why Red Doesn't Sound Like a Bell: Understanding the feel of consciousness*. Oxford University Press, 2011.

[8] S. A. Morris, *Topology without tears*, 2020.

[9] A. Censi, "Bootstrapping vehicles: A formal approach to unsupervised sensorimotor learning based on invariance," Ph.D. dissertation, California Institute of Technology, June 2012.

[10] D. Philipona, J. K. O'Regan, and J.-P. Nadal, "Is there something out there?: Inferring space from sensorimotor dependencies," *Neural Comput.*, vol. 15, no. 9, pp. 2029–2049, 2003.

[11] A. Laflaquière, J. K. O'Regan, S. Argentieri, B. Gas, and A. Terekhov, "Learning agents spatial configuration from sensorimotor invariants," *Robotics and Autonomous Systems*, vol. 71, pp. 49–59, September 2015.

[12] A. Laflaquiere, "Grounding the experience of a visual field through sensorimotor contingencies," *Neurocomputing*, vol. 268, no. C, 2017.

[13] A. V. Terekhov and J. K. O'Regan, "Space as an invention of active agents," *Frontiers in Robotics and AI*, vol. 3, p. 4, 2016. [Online]. Available: https://www.frontiersin.org/article/10.3389/frobt.2016.00004

[14] V. Marcel, S. Argentieri, and B. Gas, "Building a sensorimotor representation of a naive agent's tactile space," *IEEE Transactions on Cognitive and Developmental Systems*, vol. 9, no. 2, pp. 141–152, June 2017.

[15] V. Marcel, S. Argentieri, and B. Gas, "Where do i move my sensors? emergence of a topological representation of sensors poses from the sensorimotor flow," *IEEE Transactions on Cognitive and Developmental Systems*, pp. 1–1, 2019.

[16] J.-M. Godon, S. Argentieri, and B. Gas, "A formal account of structuring motor actions with sensory prediction for a naive agent," *Frontiers in Robotics and AI*, vol. 7, p. 179, 2020. [Online]. Available: https://www.frontiersin.org/article/10.3389/frobt.2020.561660

[17] D. Pierce and B. J. Kuipers, "Map learning with uninterpreted sensors and effectors," *Artificial Intelligence*, vol. 92, no. 1, pp. 169–227, 1997.

[18] L. A. Olsson, C. L. Nehaniv, and D. Polani, "From unknown sensors and actuators to actions grounded in sensorimotor perceptions," *Connection Science*, vol. 18, no. 2, pp. 121–144, 2006.

[19] N. Le Hir, O. Sigaud, and A. Laflaquière, "Identification of invariant sensorimotor structures as a prerequisite for the discovery of objects," *Frontiers in Robotics and AI*, vol. 5, p. 70, 2018.

[20] A. Laflaquière, S. Argentieri, O. Breysse, S. Genet, and B. Gas, "A non-linear approach to space dimension perception by a naive agent," in *Intelligent Robots and Systems (IROS), 2012 IEEE/RSJ International Conference on*, Oct 2012, pp. 3253–3259.

[21] J. L. Elman, "Finding structure in time," *Cognitive Science*, vol. 14, no. 2, pp. 179–211, 1990. [Online]. Available: https://www.sciencedirect.com/science/article/pii/036402139090002E

[22] J. Mcclelland, *Explorations in parallel distributed processing: A handbook of models, programs, and exercises*, 2nd ed., Dec. 2015. [Online]. Available: https://web.stanford.edu/group/pdplab/pdphandbook/handbook.pdf

[23] J.-M. Godon, "A structuralist formal account for sensorimotor contingencies in perception," Ph.D. dissertation, Sorbonne Université, 2022.

[24] E. W. Dijkstra *et al.*, "A note on two problems in connexion with graphs," *Numerische mathematik*, vol. 1, no. 1, pp. 269–271, 1959.

[25] J. B. Kruskal, "Nonmetric multidimensional scaling: A numerical method," *Psychometrika*, vol. 29, no. 2, pp. 115–129, 1964.

[26] ——, "Multidimensional scaling by optimizing goodness of fit to a nonmetric hypothesis," *Psychometrika*, vol. 29, no. 1, pp. 1–27, 1964.

[27] I. Borg and P. J. Groenen, *Modern multidimensional scaling: Theory and applications*. Springer Science & Business Media, 2005.

[28] J. B. Tenenbaum, V. d. Silva, and J. C. Langford, "A global geometric framework for nonlinear dimensionality reduction," *Science*, vol. 290, no. 5500, pp. 2319–2323, 2000.

[29] D. Endres and J. Schindelin, "A new metric for probability distributions," *IEEE Transactions on Information Theory*, vol. 49, no. 7, pp. 1858–1860, 2003.

[30] S. Kullback and R. A. Leibler, "On information and sufficiency," *Annals of Mathematical Statistics*, vol. 22, no. 1, pp. 79–86, March 1951.

[31] D. H. Ballard and R. Zhang, "The hierarchical evolution in human vision modeling," *Topics in Cognitive Science*, vol. 13, no. 2, pp. 309–328, 2021.